Carbon incorporation for strain compensation during solid phase epitaxial recrystallization of SiGe on Si at 500–600 °C

M. J. Antonell and K. S. Jones
Department of Materials Science and Engineering, University of Florida, Gainesville, Florida 32611

T. E. Haynes
Solid State Division, Oak Ridge National Laboratory, Oak Ridge, Tennessee 37831

(Received 6 November 1995; accepted for publication 16 February 1996)

Transmission electron microscopy has been combined with time-resolved reflectivity and ion channeling to study the effects of carbon doping on solid-phase epitaxial regrowth (SPER) of strained 2000 Å, $Si_{0.88}Ge_{0.12}Si$ alloy layers grown by molecular-beam epitaxy (MBE). Relative to the undoped layers, carbon incorporation in the MBE grown SiGe layers prior to regrowth at moderate temperatures (500–700 °C) has three main effects on SPER. These include a reduction in SPER rate, a delay in the onset of strain-relieving defect formation, and a sharpening of the amorphous/crystalline (*a*/*c*) interface, i.e., promotion of a two-dimensional (planar) growth front. These results suggest that C incorporated during SPER reduces the lattice-mismatch strain. © *1996 American Institute of Physics*. [S0021-8979(96)10310-5]

I. INTRODUCTION

$Si_{1-x}Ge_x$/Si alloys have been used for a variety of high performance electronic device applications such as heterojunction bipolar transistors (HBTs),[1–5] high mobility transistors (HMTs),[6] heterojunction field effect transistors (HFETs),[7–10] and photodetectors.[11,12] The addition of germanium to silicon allows the resulting SiGe layer to have a reduced band gap. When this layer is used as the base region of bipolar devices, the resulting band gap reduction provides several advantages, including higher emitter injection efficiency, lower base resistance, faster switching times, and improved performance at low temperatures. However, a major drawback in the use of such structures for high performance electronic devices is the relatively large lattice mismatch between Si and Ge (~4%). Such a mismatch leads to the formation of strain-relieving misfit dislocations if the layer thickness exceeds a critical value. These dislocations are undesirable since they adversely affect the device properties of the material. Several methods have been proposed to alleviate this problem. For instance, the thickness of the layer can be maintained below the critical thickness so that the layer remains pseudomorphic in nature, or the addition of a buffer layer may be introduced in order to maintain a defect free active region in the device. Each of these methods limits the device design flexibility.

It has been demonstrated that the addition of a third element such as C, P, or B during molecular-beam epitaxy (MBE) of SiGe layers can reduce epitaxial strain.[12–14] In this scheme, atoms with smaller atomic radii are introduced during growth. The addition of these elements, in the correct amounts, reduces the normal strain buildup by the formation of a ternary alloy that is matched to the Si substrate. The advantage of such an alloy is that the fabricated epilayer is stable, hence there will be no further degradation during subsequent processing steps. Thus, defect formation can be controlled and high-quality devices fabricated.

Recently the approach of forming a ternary SiGeC alloy has also been applied using ion implantation technology and initial results have been encouraging.[15,16] During processing of devices, implantation induced amorphization, and subsequent regrowth are critical steps for improving dopant activation and reducing random channeling tails. These steps offer the opportunity of introducing carbon during the normal dopant implantation for the purpose of strain compensation. Such a procedure may be expected to improve the quality of the regrown layer upon annealing without a substantial increase in the number of processing steps. In the present work, we have introduced carbon by ion implantation into strained, MBE-grown $Si_{0.88}Ge_{0.12}$ epilayers previously amorphized by ion implantation. The influence of C on the solid-phase epitaxial recrystallization (SPER) in these strained layers has been examined as a function of concentration and depth of the implanted C. Effects on the regrowth rate, microstructure, and strain are described. Reduced defect densities and flatter amorphous–crystalline interfaces are observed in C implanted layers after SPER. These results suggest that the C incorporated prior to SPER can indeed compensate the strain in SiGe epilayers.

II. EXPERIMENTAL DESCRIPTION

Strained $Si_{1-x}Ge_x$ layers were grown on *p*-type 5–20 Ω cm, 4 in. (100) Si wafers at 550 °C by MBE at Texas Instruments, Inc. Rutherford backscattering (RBS), electron microprobe (EMP), and cross-sectional transmission electron microscopy (XTEM) showed the Ge fraction to be 12% and the thickness of the alloy layer to be ~2000 Å. This $Si_{0.88}Ge_{0.12}$ epilayer was amorphized to a depth of ~3000 Å (including 1000 Å of the Si substrate) by a dual-energy implant of Si^{29+} at a substrate temperature of −100 °C, with a dose of 6×10^{14} cm^{-2} at both 70 and 150 keV. A subsequent implant of 5×10^{15} cm^{-2} carbon at 30 or 45 keV was then introduced (projected ranges of ~800 or ~1200 Å, respectively). This dose was chosen in order to give a peak carbon concentration equal to one-tenth of the Ge concentration at the projected range of the carbon implant. This is the ratio

 0021-8979/96/79(10)/7646/6/$10.00

needed to match the lattice constant in a $Si_{1-x-y}Ge_xC_y$ ternary alloy to that of Si, assuming Vegard's law applies in this material system.

Furnace anneals in the 500–600 °C range permitted *in situ* time-resolved reflectivity of the solid-phase epitaxial regrowth rates, as described below. The anneals were performed in an Ar ambient following a vacuum purge.

XTEM and ion channeling were used to characterize crystal quality and defect microstructure in the regrown layers. Ion channeling measurements were made on selected samples using either 1.0 or 2.0 MeV He^+ ions, with the detector at 160° or 110° scattering angle. XTEM samples were prepared by lapping thickness to 50–100 μm and ion milling at room temperature. Microscopy was performed on a JEOL 200 CX, or, for high resolution, a JEOL 4000 FX.

The technique of time-resolved reflectivity (TRR), as described by Olson and Roth,[17] permits an *in situ* measurement of the interface position and regrowth velocity during SPER. TRR is the preferred technique due to the efficient and rapid real-time measurement of the SPER kinetics in SiGe epilayers over a large temperature range. These measurements can be made without excessive and time consuming sample preparation. The technique is based on the constructive and destructive interference generated between the reflected laser light from the amorphous/crystalline (*a*/*c*) interface and from the surface. Alternating maxima and minima in the reflected intensity occur at thickness intervals of $\lambda/4n$, where λ is the probe wavelength and n is the index of refraction in the amorphous layer. TRR measurements were made using a He–Ne laser source with a wavelength of 6328 Å. The index of refraction (n) for the amorphous $Si_{0.88}Ge_{0.12}$ layer was found to 4.65 by spectroscopic ellipsometry.[18] Reflected and incident light intensities were measured with two Si photodiodes. The samples were mounted on a low-mass molybdenum holder using heat conductive paint. After a vacuum purge and Ar fill, the sample holder was then inserted into a preheated stage. The temperature was measured by a thermocouple embedded in the sample holder. The temperature was stable to ±1 °C after an initial settling period of ~1 min.

III. RESULTS AND DISCUSSION

A. Effect of carbon on recrystallization rate

Figure 1 shows time-resolved reflectivity data taken from three $Si_{0.88}Ge_{0.12}$ layers [Figs. 1(a), 1(c), and 1(d)] and a Si sample [Fig. 1(b)], each regrown at 560 °C. Amorphization of 1000 Å of the Si substrate was useful for three reasons. First, this allows ample time for the sample temperature to stabilize before regrowth reaches the SiGe alloy. Second, this allows time for the *a*/*c* interface to sharpen within the Si substrate before reaching the Si/SiGe heterointerface.[19] Finally, a temperature check can be performed by comparing the regrowth rate in the pure silicon portion of the sample with known Si SPE velocities. The difference in the regrowth velocity in the Si portion of the plots can be attributed to a slight difference in regrowth temperature between the anneals.

Figure 1(a) is the TRR data from $Si_{0.88}Ge_{0.12}$ layer regrown at 560 °C without C. Notice that the time interval

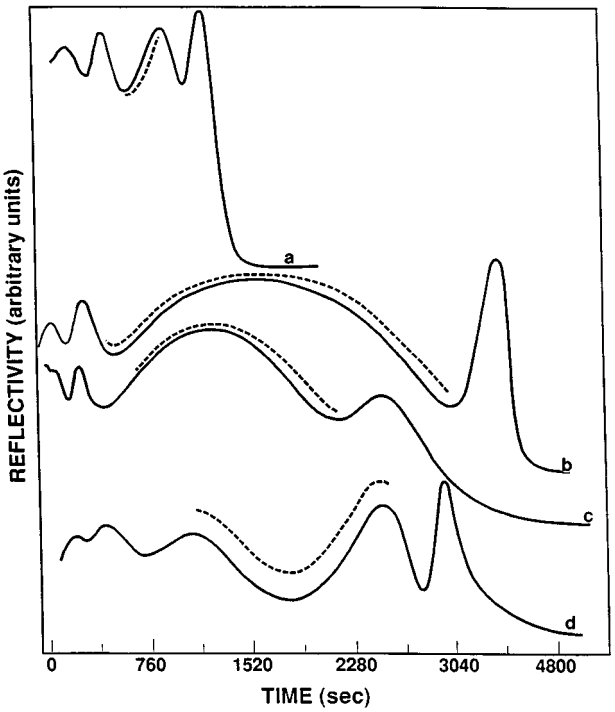

FIG. 1. Reflectivity data obtained by *in situ* regrowth of Si and SiGe alloys amorphized to a depth of 3000 Å and regrown at 560 °C. (a) 2000-Å-thick $Si_{0.88}Ge_{0.12}$/Si; (b) 30 keV carbon implanted (100)Si; (c) 30 keV carbon implanted $Si_{0.88}Ge_{0.12}Si$; (d) 45 keV carbon implanted $Si_{0.88}Ge_{0.12}$/Si.

(Δt) between peaks increases in the vicinity of the dashed line. This corresponds to a transient reduction in regrowth rate which has been described in detail by Lee, Haynes, and Jones.[20] Briefly, the decrease in regrowth rate and an increase in the SPER activation energy occurs slightly before the formation of strain-relieving defects. Strain-relieving defects begin to form in these samples at a depth of 1600 Å, with a maximum concentration at a depth of 1200 Å. The reduction in velocity and increase in activation energy prior to defect formation is believed to be a result of compressive forces acting on the lattice, since it has been shown that nonhydrostatic compressive stress retards SPER in (100) silicon.[21]

In the 30 keV carbon-implanted Si(100) sample (dose=5×10^{15} cm^{-2}), Fig. 1(b), there is also a reduction in regrowth velocity that can be recognized by the horizontally stretched peak observed between 500 and 3000 s. This reduction in velocity can be attributed to the introduction of carbon into the lattice, since carbon is known to slow SPER in silicon.[22,23] The addition of carbon increases the total regrowth time by over a factor of 2 when compared with an undoped silicon sample.

Figures 1(c) and 1(d) are data from C-doped $Si_{0.88}Ge_{0.12}$ alloy layers. The sample shown in Fig. 1(c) was implanted with a 30 keV carbon implant with a dose of 5×10^{15} cm^{-2}. These conditions result in a peak concentration of 1% carbon at a projected range of 800 Å. The sample shown in Fig. 1(d) instead had a 45 keV carbon implant, with a dose of 6×10^{15} cm^{-2}. This implant produces a similar 1% peak concentration of carbon, but at a projected range of 1200 Å, coinciding

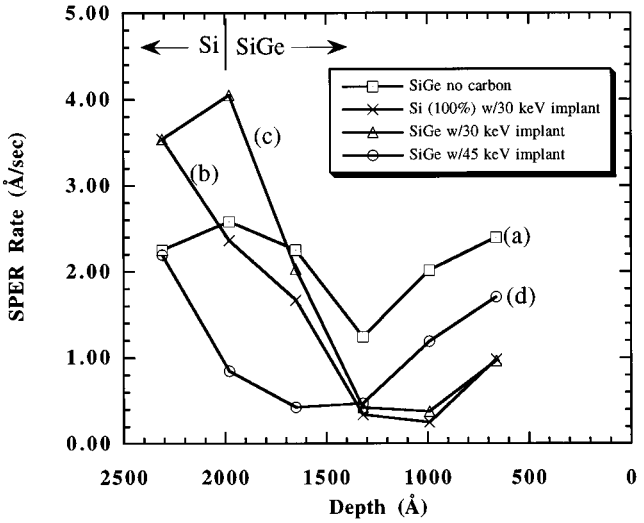

FIG. 2. Plot illustrating the change in velocity during various stages of regrowth in (a) 2000-Å-thick $Si_{0.88}Ge_{0.12}$/Si; (b) 30 keV carbon implanted (100) Si; (c) 30 keV carbon implanted $Si_{0.88}Ge_{0.12}$/Si; (d) 45 keV carbon implanted $Si_{0.88}Ge_{0.12}$/Si.

with the depth of maximum defect density in those layers regrown without carbon. As can be seen in the comparison of Figs. 1(c) and 1(d), the slowdown in the regrowth rate occurs earlier in the 45 keV implant when compared to the 30 keV implant. The earlier slowdown is consistent with the fact that the regrowing crystal encounters carbon earlier due to the deeper projected range (1200 Å) in the 45 keV carbon implant.

The regrowth rates in these layers are quantified in Fig. 2 as a function of interface depth. The SPER velocity for the undoped sample, Fig. 2(a), decreased from 2.2 Å/s prior to defect formation to 1.2 Å/s. In the carbon doped Si sample, Fig. 2(b), the velocity decreased from 1.7 Å/s before encountering carbon (~210 Å deep) to 0.25 Å/s after reaching the projected range. In the SiGe sample implanted with a 30 keV carbon implant, Fig. 2(c), the velocity decreased from 2.0 to 0.42 Å/s. The velocity also decreases similarly in the case of the 45 keV implant [Fig. 2(d)], but the minimum rate occurs deeper. The addition of carbon has decreased the regrowth velocity even further than in the undoped SiGe layers. After the *a*/*c* interface moves through the carbon profile, the SPER rates increase in all samples. We show below that the regrowth rate transients in C-implanted samples are controlled by the implant depth and are not directly correlated with defect depth as in the undoped samples.

B. Effect of carbon on defect formation

Figure 3(a) shows an XTEM micrograph from a 560 °C regrown $Si_{0.88}Ge_{0.12}$ alloy layer. The 300–400 Å nearest the Si/SiGe interface regrows relatively defect-free and is consistent with published critical thickness values.[24,25] After the initial 300–400 Å of regrowth, strain relieving defects are formed due to the lattice mismatch of the SiGe alloy layer to the silicon substrate. These strain relieving defects include stacking faults and dislocations. As can be seen in a comparison of Figs. 2(a) and 3(a), formation of defects is accompanied by a reduction in SPER velocity. These defects are preceded by a roughening of the a/c interface.[19,20]

Figure 3(b) highlights the defect formation in the Si sample with a carbon implant. Comparing Fig. 3(b) with Fig. 2(b) (the TRR curve for the carbon implanted pure silicon sample) shows that the reduction in velocity in this Si sample is clearly decoupled from the onset of defect formation, which occurs in the last 700–800 Å of regrowth.

Figure 3(c) is an XTEM micrograph of a 30 keV carbon implanted $Si_{0.88}Ge_{0.12}$ alloy layer. There is 300–400 Å of regrowth prior the onset of normal strain relieving defects just like that as seen in the undoped SiGe layer [Fig. 3(a)]. After approximately 300 Å of SiGe has regrown a high density of defects nucleate. These defects include stacking faults and threading dislocations which are periodically spaced throughout the layer, occurring every 1700 ± 100 Å. In this respect, the 30 keV C-doped layers behave very much like the undoped SiGe layers. However, in some regions near the surface, epitaxial regrowth stops and is apparently dominated by heterogeneous nucleation. This alternative recrystallization mechanism forms areas of polycrystalline material that are bound by a large density of stacking faults. These polycrystalline areas are usually located 250–300 Å from the surface termination end of a threading dislocation.

Figure 3(d) shows the analogous XTEM micrograph for a 45 keV carbon implanted $Si_{0.88}Ge_{0.12}$ alloy layer. In this sample defect formation has been delayed by about 700 Å on average relative to the undoped layer [Fig. 3(a)]. Thus there is a total of 1000–1100 Å of defect-free growth before defects form in the regrown epilayer. A comparison of Figs. 2(d) and 3(d) show that the onset of defect formation does not correspond with the retarded regrowth velocity, but occurs much later. This reduction in SPER velocity is believed to be related to the incorporation of carbon as an impurity into the lattice similarly to that observed in pure Si [Figs. 2(b) and 3(b)]. In some areas of the 45 keV sample, regrowth even reaches the surface without defect formation. However, some defects generally do grow near the surface. These defects, observed as the dark areas nearest the surface in Fig. 3(d), consist primarily of a high density of stacking fault bundles rather than the usual threading dislocations. A high resolution XTEM micrograph of such a dark region is shown in Fig. 3(e). Eventually, epitaxial regrowth within this region is overcome by heterogeneous nucleation forming polycrystalline material with some amorphous pockets.

Channeling spectra were taken to verify that the XTEM observations were indeed representative of the overall sample behavior. Figure 4 displays the Si portion of the ion channeling spectra for the four samples shown in Figs. 2 and 3. Figure 4(a) shows the channeling spectra for the $Si_{0.88}Ge_{0.12}$ samples, both with and without carbon doping, while Fig. 4(b) shows the ion channeling spectra for the carbon doped (100) silicon sample. Figure 4 (a) compares the two different carbon implants with the unimplanted $Si_{0.88}Ge_{0.12}$ sample. The channeling spectrum for the undoped sample shows a small defect-related peak near $E = 0.50$ MeV corresponding to a depth of 1200 Å. A weaker defect peak may be discernible in the spectrum from the 30

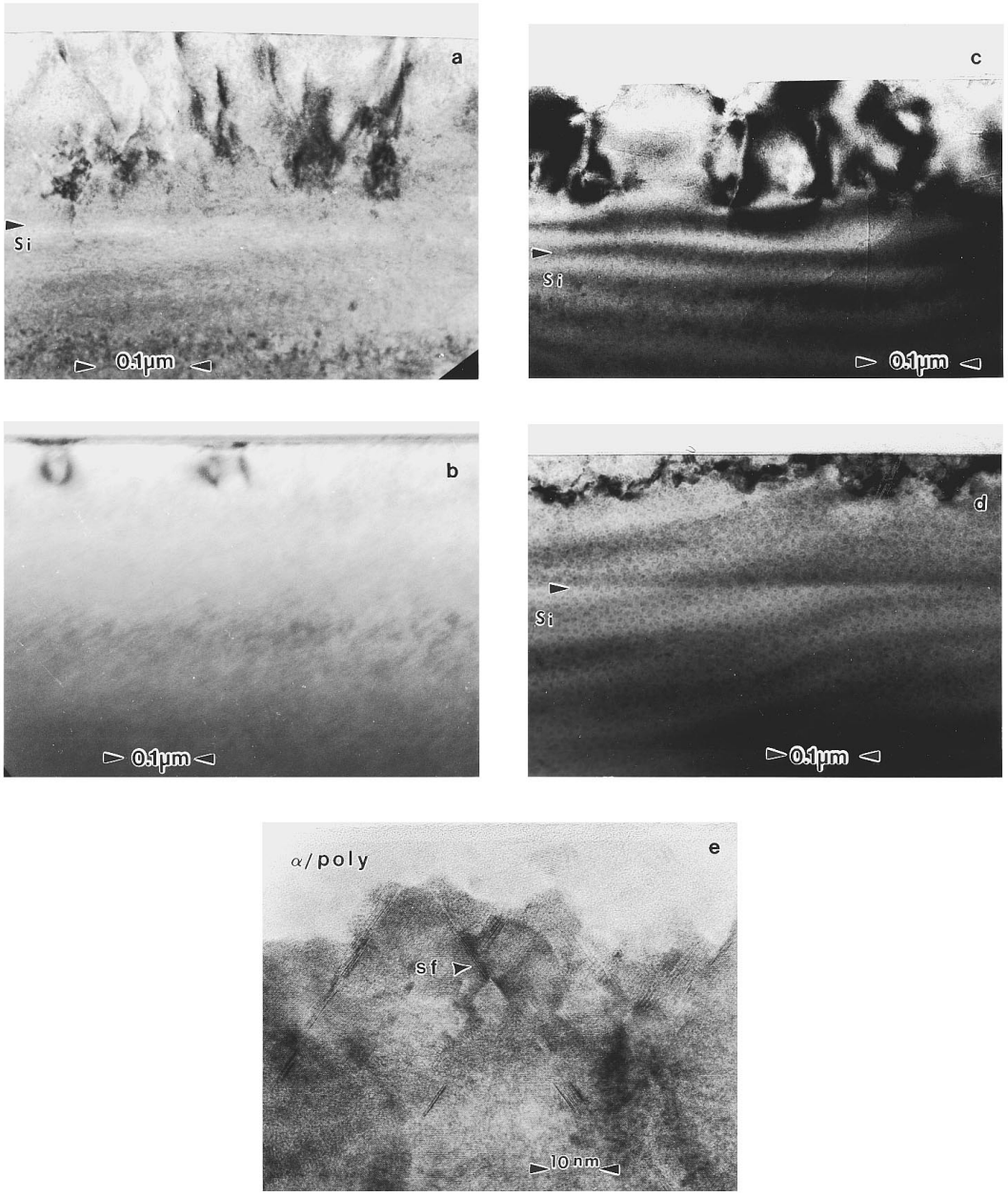

FIG. 3. Bright-field XTEM ($g=220$) image of an amorphized and regrown at 560 °C. (a) 2000-Å-thick $Si_{0.88}Ge_{0.12}$/Si; (b) 30 keV carbon implanted (100) Si; (c) 30 keV carbon implanted $Si_{0.88}Ge_{0.12}$/Si; (d) 45 keV carbon implanted $Si_{0.88}Ge_{0.12}$/Si sample, high-resolution XTEM of (e) stacking fault bundles and amorphous material located in the ''dark mass'' defects found near the surface in Fig. 3(d) [45 keV carbon implanted $Si_{0.88}Ge_{0.12}$/Si sample amorphized to a depth of 3000 Å and regrown at 560 °C].

keV C-implanted sample, but it is certainly less significant statistically. (Three spectra were taken incidentally from this same sample during the course of these experiments as a control on the ion channeling conditions, and all showed a similarly weak peak, such that we believe that this peak is real albeit very small.) No such peak can be distinguished in the 45 keV implant. However, the 45 keV carbon implanted $Si_{0.88}Ge_{0.12}$ sample has a larger surface peak than either the 30 keV carbon implant or the undoped sample. Dechanneling of the analysis beam in this surface layer [polycrystalline and amorphous pockets in Figs. 3(d) and 3(e)] masks the overall layer quality in the deeper regions, which is actually better in the 45 keV carbon implanted sample based on XTEM observations. Figure 4(b) shows the channeling spectrum from C-implanted Si. A large surface peak can be seen on this channeling spectrum corresponding to the defect formation near the surface of the silicon after annealing. The low slope to the left of the surface peak indicates a good quality regrown layer beyond the projected range of the carbon implant. Generally, these ion channeling spectra confirm the qualitative observations made from the XTEM micrographs in Fig. 3.

C. Interface roughness

Since the critical thickness for defect formation has apparently been increased by the 45 keV implant we might

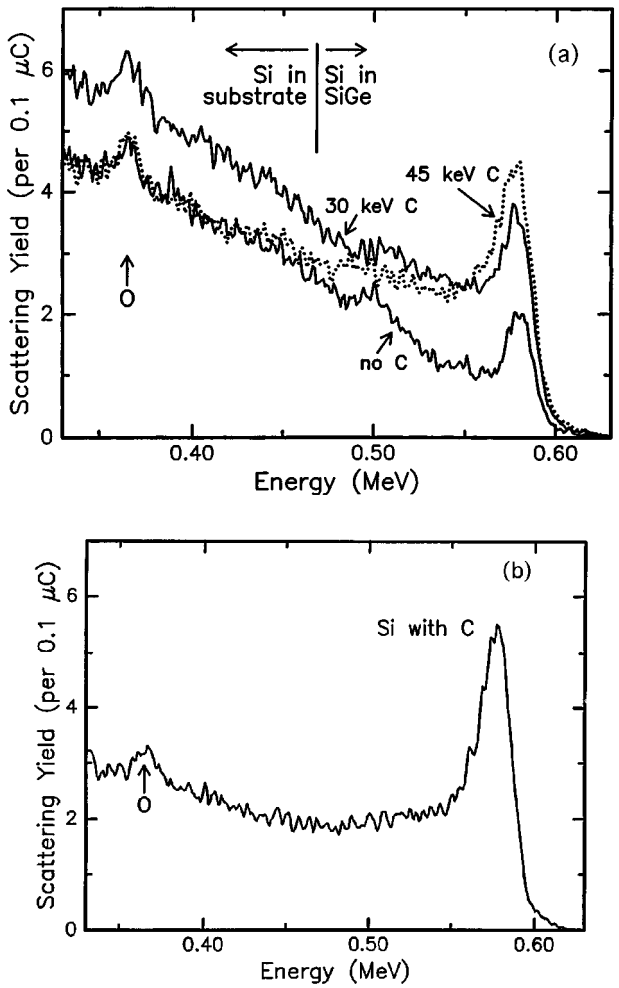

FIG. 4. The Si portion of the RBS channeling spectra obtained from (a) 2000-Å-thick $Si_{0.88}Ge_{0.12}$/Si, 30 keV carbon implanted 2000-Å-thick $Si_{0.88}Ge_{0.12}$/Si, and 45 keV carbon implanted 2000-Å-thick $Si_{0.88}Ge_{0.12}$/Si; (b) 30 keV carbon implanted into (100) Si after a 560 °C regrowth.

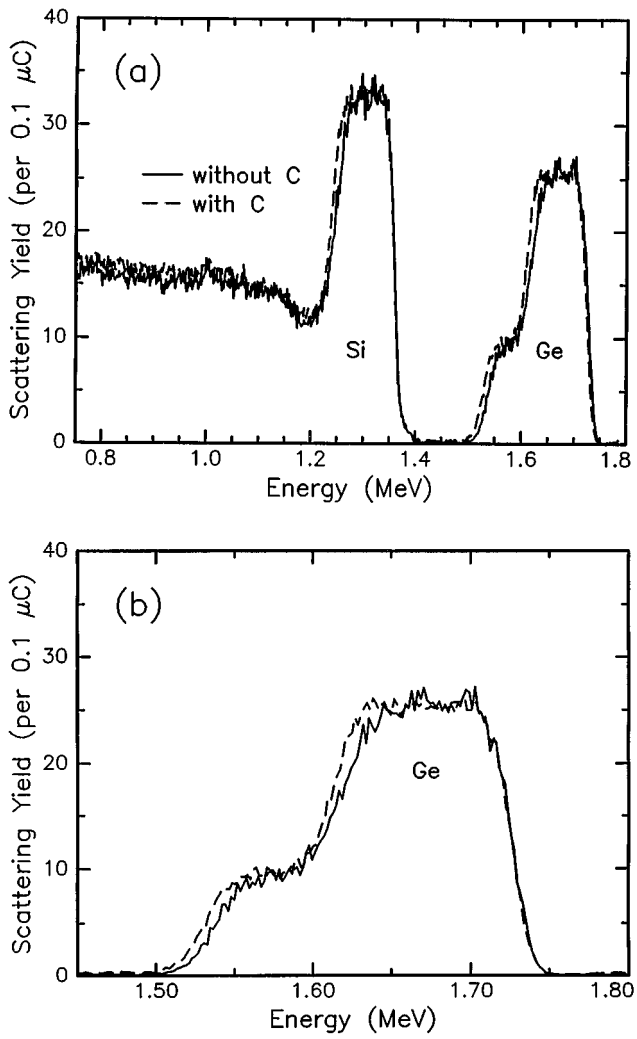

FIG. 5. RBS channeling spectra obtained from the partial regrowth of (a) an undoped 2000-Å-thick $Si_{0.88}Ge_{0.12}$/Si layer and a 30 keV implanted carbon sample into a 2000-Å-thick $Si_{0.88}Ge_{0.12}$/Si; (b) a blowup of the Ge portion of the RBS spectra illustrating the planarity of the interface by the difference in slope of the two back edges of the Ge profiles.

infer that a large part of the mismatch strain was compensated by the implanted carbon. Direct measurement of the residual strain is not possible due to the nature of the near surface defects. However, indirect evidence of strain compensation may be obtained by examining the interface roughness during SPER since strain is known to cause interface roughening.[19,20] For this test, regrowth was interrupted in some samples and the planarity of the a/c interface was determined.

Figure 5(a) shows ion channeling spectra of the C-doped and undoped $Si_{0.88}Ge_{0.12}$ alloys which have been partially regrown at 560 °C while being monitored *in situ* by TRR. Both of these samples were removed from the heater block when the thickness of SiGe was approximately 1200 Å, as determined by the TRR signal. The ion channeling in Fig. 5 was done at 2.0 MeV and the detector angle was decreased to 110° to enhance depth resolution. The flat portions of the spectra located at 1.25 to 1.35 MeV (Si signal) and 1.63 to 1.73 MeV (Ge signal) correspond to the amorphous region of the partially regrown-epilayers. Energies below 1.15 MeV contain the portion of the spectra associated with the Si substrate. Comparing the back edge of the amorphous layer in the Ge profiles shown in Fig. 5(b), it is apparent that the spectrum from the C-doped sample has a steeper slope in the 1.6–1.65 MeV region. The slope of the back edge of the channeling spectrum is proportional to the abruptness of the interface, such that the larger slope indicates a sharper interface. To make a quantitative estimate of roughness, we considered three contributions to the interface slope: (a) instrumental resolution; (b) energy straggling; and (c) interface roughness. Instrumental resolution can be determined from the slope of the high energy edge of the Ge spectrum and straggling can be estimated from the slope of the low-energy edge at 1.53 MeV (straggling is proportional to the square root of depth). After subtracting these two contributions from the slope at the *a–c* interface, it was determined that the standard deviation of the interface depth was 40 Å in the carbon implanted samples as compared to nearly 80 Å in the undoped sample. Therefore, it was concluded from this experiment that the roughness in the *a/c* interface can be sub-

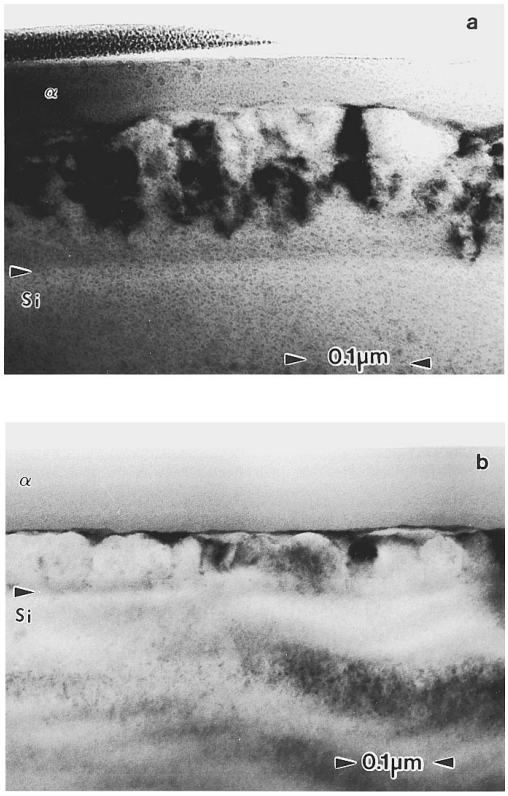

FIG. 6. Bright-field images of the 2000-Å-thick $Si_{0.88}Ge_{0.12}$ alloy layer partially regrown at 560 °C (a) without carbon; (b) with a 30 keV carbon implant.

stantially reduced with the incorporation of carbon during regrowth.

The channeling measurement of interface roughness was also confirmed by XTEM. Figure 6(a) is an XTEM micrograph of a partially regrown, undoped, SiGe sample similar to that in Fig. 5 (solid line spectrum). This sample exhibits again the typical 300–400 Å of defect-free regrowth beyond the SiGe/Si heterointerface. The remaining crystalline portion of the sample contains threading dislocations and stacking faults. It can be clearly seen that the *a*/*c* interface is very rough, with interface depths ranging between the extremes of 250 to 800 Å below the surface. The carbon doped SiGe sample shown in Fig. 6(b) illustrates a much more planar a/c interface. The interface roughness varies only by 100–150 Å when carbon is added to the SiGe by implantation. Since roughening of the *a*/*c* interface is believed to be stress-driven, it can be inferred that the stress may have been at least partially accommodated by the introduction of carbon.

IV. CONCLUSIONS

Carbon doping by ion implantation in amorphous SiGe layers has been demonstrated to delay the onset of strain-relieving defects during SPER. Defect formation that normally begins after 300–400 Å of regrowth in a sample of $Si_{0.88}Ge_{0.12}$ that has not been doped with carbon can be delayed on average an additional 600–700 Å with the addition of a 1% carbon implant. Carbon has also been shown both by ion channeling and XTEM to help maintain a two-dimensional crystalline–amorphous interface during regrowth. These two results indicate that C can be incorporated during SPER of mismatched SiGe layers on Si to reduce strain, and extend the defect-free thickness range. However, the carbon must be implanted at an optimum projected range to provide this benefit. This range must coincide with the onset of defect generation. The projected range of the 30 keV carbon implant (800 Å) was too shallow to prevent the formation of strain-relieving defects. Apparently, after the defects have formed, the carbon implant is not effective to prevent further growth.

The addition of carbon dramatically increases the time necessary for the SPER process to take place in the alloy layer. Unlike in the undoped case, this slowdown is uncoupled from defect formation. The extra time required for SPER, perhaps coupled with the introduction of impurity C, seems to enhance the likelihood of heterogeneous nucleation, resulting in polycrystalline growth near the surface.

ACKNOWLEDGMENTS

Research performed at Oak Ridge National Laboratory was sponsored by the U.S. Department of Energy, Division of Materials Sciences, under Contract No. DE-AC05-84 OR21400 with Lockheed Martin Energy Systems Inc. Work at the University of Florida was supported by NASA and the SURA/ORNL Summer Cooperative Research Program.

[1] J. C. Bean, Proc. IEEE **80**, 571 (1992).
[2] G. L. Patton and J. H. Comfort IEEE Electron Device Lett. **11**, 171 (1990).
[3] D. J. Roulston, and J. M. McGregor, Solid State Electron. **35**, 1019 (1992).
[4] S. R. Stiffler, J. H. Comfort, C. L. Stanis, D. L. Harame, and E. D. Fresart, J. Appl. Phys. **70**, 1461 (1991).
[5] K. Kamjoo, D. K. Nayak, J. S. Park, J. C. S. Woo, and K. L. Wang, J. Appl. Phys. **69**, 6674 (1991).
[6] F. Shaffler, D. Tobben, H. J. Herzog, G. Abstreiter, and B. Hollander, Semicond. Sci. Technol. **7**, 260 (1992).
[7] C. M. Gronet, J. Appl. Phys. **61**, 2407 (1987).
[8] Y. H. Xie, E. A. Fitzgerald, D. Monroe, P. J. Silverman, and G. P. Watson, J. Appl. Phys. **73**, 8364 (1993).
[9] A. Vetter, S. J. Kovacic, J. G. Simmons, J. P. Noel, and D. C. Houghton, Solid State Electron. **36**, 1247 (1993).
[10] K. L. Wang and R. P. Karunasiri, J. Vac. Sci. Technol. **11**, 1159 (1993).
[11] V. P. Kesan, P. G. May, E. Bassous, and S. S. Iyer, IEEE Electron Device Lett. **90**, 637 (1990).
[12] T. L. Lin and E. W. Jones, IEEE Electron Device Lett. **90**, 641 (1990).
[13] K. Erbel, S. S. Iyer, S, Zollner, J. C. Tsang, and F. K. LeGoues, Appl. Phys. Lett. **60**, 3033 (1992).
[14] S. Nishikawa and T. Yamaji, Appl. Phys. Lett. **62**, 303 (1992).
[15] A. Fukami, K. Shoji, and T. Nagano, Appl. Phys. Lett. **57**, 2345 (1990).
[16] S. Lombardo, F. Priolo, and S. U. Campisano, Appl. Phys. Lett. **62**, 2335 (1993).
[17] G. L. Olson and J. A. Roth, Mater. Sci. Rep. **3**, 1 (1988).
[18] G. E. Jellison and H. H. Burke (unpublished).
[19] D. C. Paine and D. J. Howard, J. Mater. Res. **5**, 1023 (1990).
[20] C. Lee, T. E. Haynes, and K. S. Jones, Appl. Phys. Lett. **62**, 501 (1993).
[21] M. J. Aziz, P. C. Sabin, and G.-Q. Lu, Phys. Rev. **44**, 9812 (1991).
[22] D. C. Paine, N. D. Evans, and N. G. Stoffel, J. Appl. Phys. **70**, 4278 (1991).
[23] S. Isomae, T. Ishiba, T. Ando, and M. Tamura, J. Appl. Phys. **74**, 3815 (1993).
[24] D. C. Houghton, J. Appl. Phys. **70**, 2136 (1991).
[25] M. L. Green, B. E. Weir, D. Brasen, Y. F. Hsieh, G. Higashi, A. Feygenson, L. C. Feldman, and R. L. Headrick, J. Appl. Phys. **69**, 745 (1991).